Photoluminescence studies on a new red emitting Sm^{3+}-doped alkaline-earth vanadate phosphor: $Ca_3Sr_3(VO_4)_4$: Sm^{3+}, Na^+

JIAYUE SUN*, RANDI SUN, JIANFENG SUN, HAIYAN DU
College of Chemistry and Environmental Engineering, Beijing Technology and Business University, Beijing 100048, PR China

A series of new red-emitting $Ca_3Sr_{3-2x}(VO_4)_4$:$x$$Sm^{3+}$,$x$$Na^+$ phosphors were synthesized by a solid-reaction method. XRD phase analysis results indicate that the sample begins to crystallize at 800 ºC, and single-phase $Ca_3Sr_3(VO_4)_4$ is fully obtained after annealing at 1000 ºC. The as-prepared phosphors have good excitation properties in the region of 350-450 nm, which perfectly match the emission wavelength of near-UV light-emitting diodes (LEDs). Three characteristic emissions peaking at 563, 601 and 646 nm can be obtained upon 406 nm excitation with the chromaticity coordinates of (0.654, 0.321), which are due to $^4G_{5/2}$- $^6H_{5/2}$, $^4G_{5/2}$-$^6H_{7/2}$ and $^4G_{5/2}$-$^6H_{9/2}$ transitions of Sm^{3+} ions. Further, the concentration quenching and corresponding luminescence mechanisms of $Ca_3Sr_{3-2x}(VO_4)_4$: $x$$Sm^{3+}$, $x$$Na^+$ phosphors were also discussed, and the critical distance was determined to be about 7.75 Å.

(Received February 25, 2010; accepted March 16, 2011)

Keywords: Optical materials, Phosphors, White LEDs, Optical properties

1. Introduction

White light-emitting diodes (LEDs) consisting of a high-performance InGaN (gallium nitride) LED and the corresponding phosphors have come into widespread use in commercial applications. Currently, most commercially available white LEDs are based on phosphor-converted (PC) emission method. In PC LEDs devices, a blue light InGaN LED chip loaded with a yellow phosphor YAG:Ce ($(Y_{1-a}Gd_a)_3(Al_{1-b}Ga_b)_5O_{12}$:$Ce^{3+}$) to obtain white light, which is now widely used as a conventional white LEDs [1]. Alternatively, White LEDs can also be fabricated by pumping red, green and blue light-emitting phosphors coated on the near-UV LED chip, which is a focus in material and luminescence research nowadays. However, there are still some problems present in this type of White LED. For instance, the emitting efficiency of commercially available red-emitting phosphors (Y_2O_2S:Eu^{3+}, (Sr, Ca)S: Eu^{2+} and so on) is much lower than that of the blue and green phosphors ($BaMgAl_{10}O_{17}$:Eu^{2+} and ZnS:(Cu^+, Al^{3+})). Besides, these sulfide red-emitting phosphors are chemically unstable and low color-rendering index [2]. In order to overcome their drawbacks, several molybdates and tungstates have been well-investigated, such as $Gd_{2-x}MO_6$: $x$$Eu^{3+}$ (M= W, Mo) [3], $LiEuM_2O_8$ (M= Mo, W) [4], $Sr_{2-2x}CaMoO_6$: $x$$Eu^{3+}$, $x$$Na^+$ [5]. Further, we have also reported the fine-sized red-emitting $Ba_{2-x}Mg(BO_3)_2$: $x$$Eu^{2+}$ phosphors synthesized by a microwave-assisted sol-gel route [6]. Till now, the development of efficient orange or red phosphors that can be excited by around 400 nm irradiation is still a key technology for achieving the tricolor white LED lighting system.

It is accepted that Sm^{3+} ions in some proper host materials can exhibit the dominant red emission peaking at 563, 601 and 646 nm under near-UV excitation, which result from $^4G_{5/2}$- $^6H_{5/2}$, $^4G_{5/2}$-$^6H_{7/2}$ and $^4G_{5/2}$-$^6H_{9/2}$ transitions, respectively. Compare with Eu^{3+} ions, the color-rendering index on the proper host materials doped with Sm^{3+} ions is higher. Moreover, vanadate compounds are more chemically stable than those sulfide red-emitting phosphors. Until recently, $Ca_3Sr_3(VO_4)_4$ and red-emitting $Ca_3Sr_3(VO_4)_4$: Eu^{3+}, M (M = Li^+, Na^+, K^+) phosphors have been reported by S. Choi et al [7-8]. In this paper, we studied the luminescence behavior of Sm^{3+} ion activated $Ca_3Sr_3(VO_4)_4$ phosphors synthesized by the solid-state reaction method and consider the concentration quenching of Sm^{3+} in order to calculate the critical distance of the energy transfer and finally reveal the luminescence mechanisms.

2. Experimental

The phosphors were synthesized by conventional solid-state reaction. $Ca(OH)_2$ (analytical reagent, A. R.), $SrCO_3$(A. R.), V_2O_5 (A. R.), Na_2CO_3 (A. R.) and Sm_2O_3 (99.999 %) were used as the starting materials in this solid-state route. Based on the results of S. Choi's study,

[7, 8]. We considered that Sm most likely occupied the Sr position. Therefore, the raw materials for investigating the effects of Sm were mixed in molar ratios according to:

$$Ca_3Sr_{3-2x}(VO_4)_4{:}xSm^{3+},xNa^{+} \quad (1)$$

In Eq. 1, variables x were varied as x = 0.01, 0.03, 0.05, 0.10, 0.15 and 0.20. Na^+ ion was used as the charge compensatory addictive in the $Ca_3Sr_3(VO_4)_4$: Sm^{3+} phosphor. The mixtures of raw materials were thoroughly mixed in an agate mortar by grinding and then placed in a corundum crucible with a lid. They were firstly preheated at 500 ºC, for the sufficient diffuse and infiltration of the starting materials. After that, the preheated mixtures were milled sufficiently again after cooling and subsequently sintered at the selected temperatures of 800 ºC, 900 ºC, 1000 ºC and 1100 ºC for 6 h in flowing air.

The phase structure of the as-prepared phosphor was recorded by an X-ray Powder diffraction spectroscopy (XRD, Shimadzu, XRD-6000) operating at Cu Kα radiation, 40 kV, 30 mA, and a scan speed of 2.0° (2θ)/min. Diffuse reflection spectra of as-synthesized phosphor powder samples were measured on a UV-Vis-NIR spectrophotometer (UV-3600, SHIMADZU) attached to an integral sphere**,** using $BaSO_4$ as a standard measurement. The excitation and emission spectra were recorded by using a Perkin-Elmer LS-55 fluorescence spectrophotometer with a photomultiplier tube operating at 400 V, and a 150-W Xe lamp was used as the excitation lamp; the measured fluorescence spectra data were all calibrated under the same operating conditions.

3. Results and discussion

3.1 XRD analysis

Fig. 1 exhibits the XRD patterns of $Ca_3Sr_{2.8}(VO_4)_4$:$0.10Sm^{3+}$, $0.10Na^+$ phosphors annealed at different temperatures in flowing air. As shown in Fig. 1 (a), some characteristic diffraction peaks corresponding to $Ca_3Sr_3(VO_4)_4$ phase appear except for the low diffraction peaks intensities, and diffraction peaks induced by such minor phases can be indexed to the main diffraction lines of $Ca_3(VO_4)_2$ and $Sr_3(VO_4)_2$. When the sintering temperature reaches at 900 ºC, the observed characteristic diffraction peaks of $Ca_3Sr_3(VO_4)_4$ become sharper and stronger, and the impure phases decrease by degrees, which indicates the crystallinity of $Ca_3Sr_3(VO_4)_4$ increases, as seen in Fig. 1 (b). In Fig. 1 (c), it is found that single-phase $Ca_3Sr_3(VO_4)_4$ is obtained after annealing at 1000 ºC, which can be in good agreement with the standard data of $Ca_3Sr_3(VO_4)_4$ (JCPDS No. 52-0468, data not shown). This result clearly demonstrates that 1000 ºC is the appropriate crystallization temperature of the $Ca_3Sr_3(VO_4)_4$, which is in consonant with the studies of S. Choi's work [7-8]. Moreover, we have measured the XRD patterns of samples with the small amount of Sm^{3+} concentrations (x=0.01~0.20). The conclusion is that the different Sm^{3+} concentrations between 0.01 and 0.20 nearly have little influence on the $Ca_3Sr_3(VO_4)_4$ system structure, though incorporation of excessive amounts of rare earth ions (x>0.50) may lead to the formation of other solid solutions rather than $Ca_3Sr_3(VO_4)_4$ phase. On the contrary, it is found that diffraction peaks for Na^+ charge compensated phosphors are well matched to rhombohedral $Ca_3Sr_3(VO_4)_4$ (JCPDS 52-0468) with a R3c space group. According to the ion radii of Sm^{3+} (0.96 Å), Na^+ (0.97 Å) and Sr^{2+} (1.12 Å), the Sr^{2+} ion can be partly substituted by Sm^{3+} and Na^+ ions without change of $Ca_3Sr_3(VO_4)_4$ crystal structure. Moreover, when the Na^+ ion is compensated, the luminescence properties of the phosphors are more enhanced than $Ca_3Sr_{2.9}(VO_4)_4$: $0.10Sm^{3+}$.

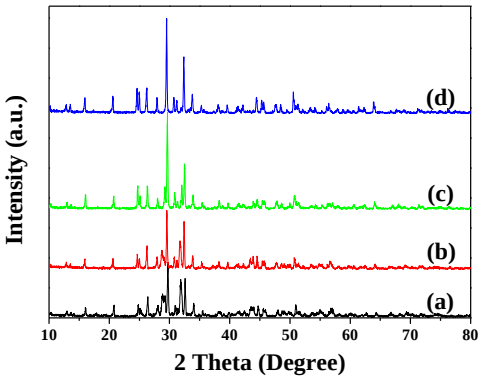

Fig. 1. X-ray diffraction patterns of $Ca_3Sr_{2.8}(VO_4)_4$: $0.10Sm^{3+}$, $0.10Na^+$ samples sintered at (a) 800 ºC, (b) 900 ºC, (c) 1000 ºC and (d) 1100 ºC for 6 h in flowing air.

3.2 Effect of sintering temperature dependence photoluminescence analysis

To investigate the energy absorption of the samples, Fig. 2 (I) gives the diffuse reflection spectra of $Ca_3Sr_{2.8}(VO_4)_4$: $0.10Sm^{3+}$, $0.10Na^+$ phosphors annealed at different temperatures. As shown in Fig. 2 (I), the broad absorption band range from 230 nm to 330 nm is observed for all compositions and this band is due to charge transfer (CT) states of VO_4^{3-} which belongs to the $^1A_1$-$^1T_1$ allowed transition [9]. Based on the molecular orbital for the VO_4^{3-} group, the overall excited state consists of increased electron density in the vicinity of the metal ion, along the tetrahedral bonds. Therefore, the allowed transition and the oscillator strength is much higher than that of usual activators [10]. Further, for the $Ca_3Sr_{2.8}(VO_4)_4$: $0.10Sm^{3+}$, $0.10Na^+$ phosphors sintered at 800 ºC and 1100 ºC [Curve a and d in Fig. 2 (I)], the onset of the reflectance is around 200 nm, and it increases slowly until up to 250 nm; Then a reflectance platform appears in the wavelength range of 260 nm to 330 nm. After that, the reflectances of the two curves decrease steeply, until up to 410 nm. It can be found that only one absorption band ranging from 210 nm to 330 nm exists in the above two curves. Another two

diffuse reflection curves of the phosphors sintered at 900 ºC and 1000 ºC [Curve b and c in Fig. 2 (I)] show the strong absorption band ranging from 310 nm to 450 nm, which demonstrates that higher temperature may contribute to the formation of the host lattice and more intense absorption of near-UV. However, too high sintering temperature may cause more reflectance and be not conducive to more intense absorption of near-UV, which has be demonstrate clearly in curve d of Fig. 2 (I). With increasing temperature, the absorption intensity of $Ca_3Sr_{2.8}(VO_4)_4$: $0.10Sm^{3+}$, $0.10Na^+$ increases and it has the maximum at 1000 ºC, then the absorption intensity decreases gradually. Further, the *inset* in Fig. 2 (I) shows the sintering temperature dependence of the PLE spectra for $Ca_3Sr_{2.8}(VO_4)_4$: $0.10Sm^{3+}$, $0.10Na^+$ phosphors by monitoring at 601 nm. For every sample, the PLE spectra consist of the broad absorption band with peak maximum at 330 nm and this is due to oxygen to vanadium CT transition in VO_4^{3-} group. Additionally, there are five obvious characteristic Sm^{3+} excitation lines in the excitation spectra, which correspond to the transitions of $^6H_{5/2}$–$^6P_{5/2}$ at 360 nm, $^6H_{5/2}$–$^4L_{17/2}$ at 374 nm, $^6H_{5/2}$–$^4F_{7/2}$ at 406 nm, $^6H_{5/2}$–$^4I_{15/2}$ at 440 nm and $^6H_{5/2}$–$^4I_{11/2}$ at 472 nm, respectively [11]. It is observed that the excitation line peaking at 406 nm has the strongest intensity. Effects of annealing temperature on the PL spectra of the $Ca_3Sr_{2.8}(VO_4)_4$: $0.10Sm^{3+}$, $0.10Na^+$ phosphors are shown in Fig. 2(II). We can see that the emission intensities increase with increasing annealing temperature, and reach a maximum at 1000 ºC, then the emission intensity decreases as the temperature further increases. Moreover, three obvious characteristic Sm^{3+} emission lines can be observed under the excitation of 601 nm, which belong to the transitions of $^4G_{5/2}$–$^6H_{5/2}$ at 563 nm, $^4G_{5/2}$–$^6H_{7/2}$ at 601 nm and $^4G_{5/2}$–$^6H_{9/2}$ at 646 nm [11]. Based on the diffuse reflection spectra, PLE and PL spectra of $Ca_3Sr_{2.8}(VO_4)_4$: $0.10Sm^{3+}$, $0.10Na^+$ phosphors for various sintering temperature, it can be observed that the absorption, excitation and emission intensities of $Ca_3Sr_{2.8}(VO_4)_4$: $0.10Sm^{3+}$, $0.10Na^+$ with different annealing temperature have the same variation trend. It can be seen that the emission intensities increase with increasing annealing temperature, and reach a maximum at 1000 ºC. Then the emission intensity decreases as the temperature further increases, which may be due to the temperature quenching [12].

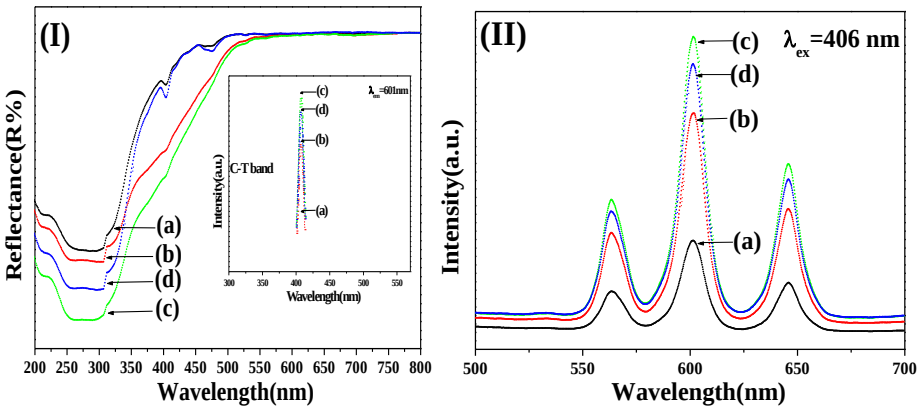

Fig. 2. (I) Diffuse reflection spectra of $Ca_3Sr_{2.8}(VO_4)_4$: $0.10Sm^{3+}$, $0.10Na^+$ phosphors for various calcination temperature, (a) 800 ºC, (b) 900 ºC, (c) 1000 ºC and (d) 1100 ºC, and the inset shows the corresponding PLE spectra (λ_{em}= 601 nm). (II) PL spectra (λ_{ex} = 406 nm) of $Ca_3Sr_{2.8}(VO_4)_4$: $0.10Sm^{3+}$, $0.10Na^+$ phosphors for various calcination temperature, (a) 800 ºC, (b) 900 ºC, (c) 1000 ºC and (d) 1100 ºC.

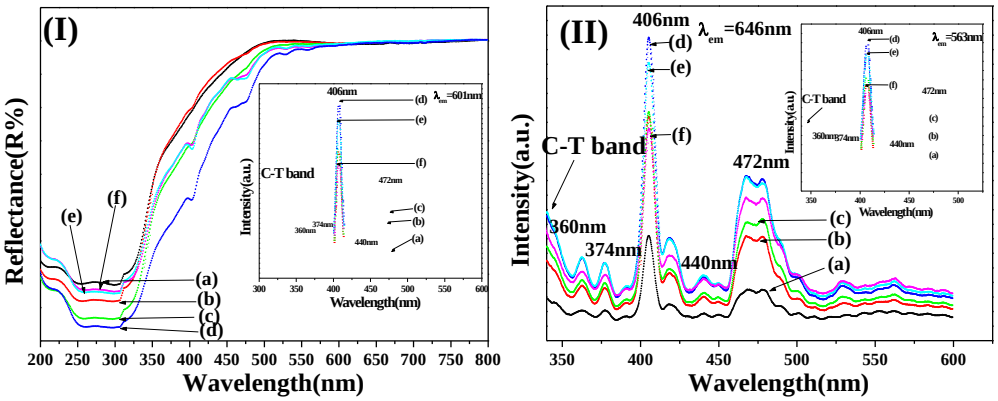

Fig. 3. Diffuse reflection spectra (I) and PLE spectra (λ_{em} = 646 nm) (II) of $Ca_3Sr_{3-2x}(VO_4)_4$: xSm^{3+}, xNa^+ phosphors obtained at 1000 ºC for various Sm^{3+} concentrations, (a) x = 0.01, (b) x = 0.03, (c) x = 0.05, (d) x = 0.10, (e) x = 0.15 and (f) x = 0.20; The inset in (I) shows the corresponding PLE spectra (λ_{em}= 601 nm), and the inset in II) represented the PLE spectra by monitoring at 563 nm.

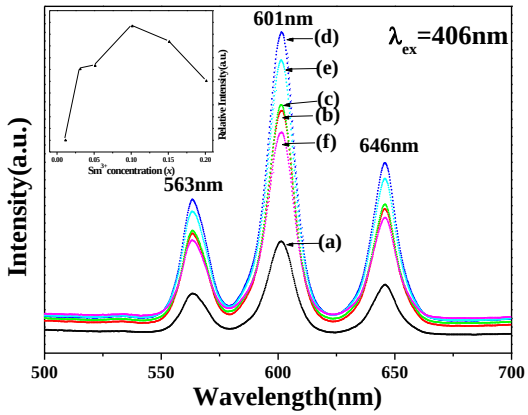

Fig. 4. PL spectra (λ_{ex} = 406 nm) of $Ca_3Sr_{3-2x}(VO_4)_4$: xSm^{3+}, xNa^+ phosphors obtained at 1000 ºC for various Sm^{3+} concentrations, (a) x = 0.01, (b) x = 0.03, (c) x = 0.05, (d) x = 0.10, (e) x = 0.15 and (f) x = 0.20; The inset represented the Sm^{3+} emission intensities at 601 nm as a function of Sm^{3+} concentration (x).

3.3 Effect of Sm^{3+} concentration dependence photoluminescence analysis

It is generally accepted that effect of Sm^{3+} concentration plays an important role in the luminescence properties of the red-emitting phosphor. Therefore, the variations of optical properties with different Sm^{3+} concentration for $Ca_3Sr_{3-2x}(VO_4)_4$: xSm^{3+}, xNa^+ phosphors have been investigated in this paper. Fig. 3 (I) gives the diffuse reflection spectra of the compounds $Ca_3Sr_{3-2x}(VO_4)_4$: xSm^{3+}, xNa^+ (x = 0.01, 0.03, 0.05, 0.10, 0.15 and 0.20) prepared at 1000 °C for 6 h with different Sm^{3+}-doping concentrations, which are recorded under the same experimental conditions. All the samples corresponding to the five Sm^{3+} concentrations' compositions show broad absorption band in the wavelength range of 230 nm to 450 nm, and this band is due to oxygen to vanadium CT transition in VO_4^{3-} group, the same as discussed previously above. The *inset* of Fig. 3(I) gives the PLE spectra of $Ca_3Sr_{3-2x}(VO_4)_4$: xSm^{3+}, xNa^+ phosphors with varied Sm^{3+} dopant concentration, by monitoring the $^4G_{5/2}$–$^6H_{7/2}$ transition of Sm^{3+} at 601 nm. Similar to the *inset* in Fig. 2 (I), five obvious characteristic Sm^{3+} excitation lines can be observed in the excitation spectra, which belong to the transitions of $^6H_{5/2}$–$^6P_{5/2}$ at 360 nm, $^6H_{5/2}$–$^4L_{17/2}$ at 374 nm, $^6H_{5/2}$–$^4F_{7/2}$ at 406 nm, $^6H_{5/2}$–$^4I_{15/2}$ at 440 nm and $^6H_{5/2}$–$^4I_{11/2}$ at 472 nm, respectively. In addition, CT transition peaking at 330 nm can be observed in the PLE spectra. Similar characteristic excitation lines and CT transition band can also be found in the PLE spectra of Fig. 3 (II) and the *inset*, which are monitored by the emission wavelength of 646 and 563 nm. In relation with Fig. 3 (I) and (II), we can also conclude that the $Ca_3Sr_{2.8}(VO_4)_4$: $0.10Sm^{3+}$, $0.10Na^+$ phosphor has the strongest absorption in the PLE spectra, which is found to be consistent with those observed in the diffuse reflection spectra.

Fig. 4 shows the dependence of the PL spectra of Sm^{3+} on its doping concentration (x) in the $Ca_3Sr_{3-2x}(VO_4)_4$: xSm^{3+}, xNa^+ (x = 0.01, 0.03, 0.05, 0.10, 0.15 and 0.20) phosphors. The emission spectra are composed of a variety of sharp line emissions corresponding to $^4G_{5/2}$–$^6H_{5/2}$ at 563 nm, $^4G_{5/2}$–$^6H_{7/2}$ at 601 nm and $^4G_{5/2}$–$^6H_{9/2}$ at 646 nm, which are characteristic emission transitions of Sm^{3+}. With different Sm^{3+} concentrations, the PL spectra have no significant changes except for the emission intensity. Further, concentration quenching of the luminescence for $Ca_3Sr_{3-2x}(VO_4)_4$: xSm^{3+}, xNa^+ phosphors can also be observed in the *inset* of Fig. 4. As the Sm^{3+} concentration increases, the emission intensity increases, and it maximizes at about x = 0.10. We propose that concentration quenching occurs, when the Sm^{3+} concentration is beyond x = 0.10.

In general, the concentration quenching of the luminescence is due to the energy transfer from one activator to another until all the energy is consumed. For this reason, it is necessary to obtain the critical distance (R_c) that is the critical separation between the donor (activator) and acceptor (quenching site). Hence, we have calculated the critical distance for energy transfer by using the relation given by Blasse [13]:

$$R_c \approx 2\left(\frac{3V}{4\pi x_c N}\right)^{\frac{1}{3}} \qquad (2)$$

Where V is the volume of the unit cell, x_c is the critical concentration of activator ion, and Z is the number of formula units per unit cell. According to S. Choi's study on the structure of the $Ca_3Sr_3(VO_4)_4$ compound [7], it has a rhombohedral phase, its cell volume (V) is 4086.91 Å^3, and the Z ions are 21. Considering the critical concentration is 0.10, the critical transfer distance of Sm^{3+} in $Ca_3Sr_3(VO_4)_4$: Sm^{3+}, Na^+ phosphor is found to be about 7.75 Å.

Further, the Commission International del'Eclairage (CIE) chromaticity coordination of the $Ca_3Sr_{2.8}(VO_4)_4$:$0.10Sm^{3+}$,$0.10Na^+$ phosphor has been calculated from the PL spectra under the excitation of 406 nm. The chromaticity coordinates (x, y) of this phosphor are (0.654, 0.321). The characteristic index shows that the $Ca_3Sr_{2.8}(VO_4)_4$: $0.10Sm^{3+}$, $0.10Na^+$ phosphor has an intense red emission. Therefore the $Ca_3Sr_3(VO_4)_4$: Sm^{3+}, Na^+ phosphor could be a potential suitable red-emitting phosphor candidate for white LEDs.

4. Conclusions

In summary, a series of $Ca_3Sr_{3-2x}(VO_4)_4$: xSm^{3+}, xNa^+ red-emitting phosphors were prepared by the

solid-reaction method. The crystallization process, structure and luminescence characteristics of the $Ca_3Sr_{3-2x}(VO_4)_4$: $x$$Sm^{3+}$, $x$$Na^+$ phosphors were investigated in detail. Results indicated that $Ca_3Sr_{2.8}(VO_4)_4$: $0.10Sm^{3+}$, $0.10Na^+$ phosphor synthesized at 1000 ºC exhibited the characteristic excitation lines of Sm^{3+} ion extending from 320 nm to 470 nm and three characteristic sharp line emissions can be observed, corresponding to $^4G_{5/2}$–$^6H_{5/2}$ at 563 nm, $^4G_{5/2}$–$^6H_{7/2}$ at 601 nm and $^4G_{5/2}$–$^6H_{9/2}$ at 646 nm. Moreover, concentration quenching mechanisms of $Ca_3Sr_{3-2x}(VO_4)_4$: $x$$Sm^{3+}$, $x$$Na^+$ phosphors were discussed. The result of theoretical calculation suggested that the critical distance of the energy transfer in the phosphor was determined to be about 7.75 Å. Finally, *CIE* chromaticity coordination of the $Ca_3Sr_{2.8}(VO_4)_4$: $0.10Sm^{3+}$, $0.10Na^+$ phosphor was calculated by the PL spectra under 406 nm excitation, viz, (0.654, 0.321). In view of its characteristic excitation band in the near-UV region, intense red emission, this phosphor could be a promising candidate for near-UV white LEDs.

Acknowledgements

This work was supported by the National Natural Science Foundation of China (No. 20876002), the Beijing Natural Science Foundation (No. 2091002, and No. 2082009), and Funding Project for Academic Human Resources Development in the Institution of Higher Learning Under the Jurisdiction of Beijing Municipality.

References

[1] R. Muller-Mach, G.O. Mueller, IEEE J. Sel. Top. Quantum Electron., **8**, 339 (2002).
[2] Z. Wang, H. Liang, L. Zhou, H. Wu, M. Gong, Q. Su. Chem. Phys. Lett., **412**, 313 (2005).
[3] F. Lei, B Yan, H Chen, J. Solid State Chem., **181**, 2845 (2008).
[4] J. Wang, X. Jing, C. Yan, J. Lin, F. Liao, J.Lumin., **121**, 57 (2006).
[5] Z. Xia, J. Sun, H. Du, D. Chen, J. Sun, J. Mater. Sci., **45**, 1553 (2010).
[6] H. Du, J. Sun, Z. Xia, J. Sun, J. Electrochem. Soc., **156**, J361 (2009).
[7] S. Choi, Y. Moon, K. Kim, H. Jung, S. Nahm, J. Lumin. **129**, 988 (2009).
[8] S. Choi, Y. Moon, H. Jung, Mater. Res. Bull.**45**, 118 (2010).
[9] K. Park, S. Mho, J. Lumin. **95**, 122 (2007).
[10] M. Anitha, P. Ramakrishnan, A. Chatterjee, G. Alexander, H. Singh, Appl. Phys. A **153**, 74 (2002).
[11] Y. Won, H. Jang, W. Im, D. Jeon, J. Electrochem. Soc., **155**, J226 (2008).
[12] W. Ding, J. Wang, Mei Zhang, Q. Zhang, Q. Su, Chem. Phys. Lett., **435**, 301 (2007).
[13] G. Blasse, J. Solid State Chem., **62**, 207 (1986).

*Corresponding author: jiayue_sun@126.com